Room temperature aqueous phase synthesis and characterization of novel nano-sized coordination polymers composed of copper(II), nickel(II), and zinc(II) metal ions with *p*-phenylenediamine (PPD) as the bridging ligand

Rimpy Gupta[1]
Email: rimpygupta84@gmail.com

Sumit Sanotra[1]
Email: sumitsanotra14@rediffmail.com

Haq Nawaz Sheikh[1*]
[*] Corresponding author
Email: hnsheikh@rediffmail.com

Bansi Lal Kalsotra[1]
Email: blkalsotra@rediffmail.com

[1] Post-Graduate Department of Chemistry, University of Jammu, Jammu Tawi 180006, India

Abstract

Nanostructured metal-organic hybrid materials composed of nickel(II), copper(II), and zinc(II) metal ions and *p*-phenylenediamine (PPD) as the organic ligand were synthesized in aqueous medium at room temperature. The synthesized compounds were characterized by elemental analyses, powder X-ray diffraction (PXRD) spectra, Fourier transform infrared spectra, nuclear magnetic resonance (^{1}H NMR) spectra, electronic spectra, scanning electron microscopy, N_2 adsorption-desorption isotherm, and dynamic light scattering studies. N_2 adsorption-desorption isotherm of copper(II)-PPD compound confirmed that it has mesoporous structure as it exhibits type-IV reversible isotherm with *H1* hysterisis. Steep adsorption indicated that the mesopores possessing it are of uniform order. Barrett-Joyner-Halenda model showed an average pore diameter of 5.2 nm. The PXRD patterns of all the three compounds are identical and showed well-defined and highly intense diffraction peaks, thereby suggesting their nature as crystalline. The broadness of the diffraction peaks indicated that the particles are of nanometer dimensions.

Keywords

Nanostructured, *p*-Phenylenediamine, Aqueous medium, Mesoporous, Crystalline

Background

Metal-organic frameworks (MOFs) are a new development in the interface between molecular coordination chemistry and material science. They are a class of porous polymeric material consisting of metal ions linked together by organic bridging ligands. Metal-organic hybrid materials have been used for ion exchange, gas adsorption, catalysis and enantio-selective separations [1,2]. Using different metal ions and selecting special organic ligands, a variety of metal-organic hybrid materials with significant new structures and properties have been synthesized [3,4].

So far, most studies on the synthesis of the metal-organic hybrid materials have focused on obtaining large crystal structures. In principle, if metal-organic materials can be obtained at a nanoscale, the surface area of the materials will be larger, and the quantum mechanical effects such as the 'quantum size effect' begin to play a significant role. These effects play minor role when going from macro to micro dimensions but become increasingly important when nanometer size range is reached [5-9]. Scaling down these materials to the nanoregime has enabled their use in a broad range of applications including catalysis, spin-crossover, templating, biosensing, biomedical imaging, and anticancer drug delivery [10-12].

However, researchers have not paid enough attention to the significance of syntheses of the metal-organic hybrid nanomaterials. Some hybrid nanomaterials have been reported [10,13,14]. Phenylenediamine (PPD) has been proven as a good building block for the synthesis of the inorganic–organic structures [15,16]. The $[CuCl_4{-}(H_2L)]$ (L=*p*-phenylenediamine) has been synthesized in strong acidic condition and identified as having a layered structure in which the hydrogen bonding plays an important role [15]. Sun and others have successfully synthesized submicrometer-scale, monodisperse spherical colloids of coordination polymers from the mixture of H_2PtCl_6 and *p*-phenylenediamine (PPD) aqueous solutions at room temperature [17]. The influence of molar ratio and concentration of reactants on such colloids was investigated, and the optimum experimental parameters for the formation of monodisperse products were proposed [17]. Based on these studies, we have tried to synthesize some functional MOF nanomaterials using PPD as the organic ligand. In this study, we report on three new hybrid nanostructures composed of nickel(II), copper(II), and zinc(II) with *p*-phenylenediamine as the organic ligand. Such hybrid nanostructures with versatile properties provoked by combining the merits of both organic as well as inorganic part may find applications in many fields [18-20].

Various attempts to obtain single crystals of synthesized polymers have so far been unsuccessful. The polymers have been characterized by elemental analyses, powder X-ray diffraction (PXRD), Fourier transform infrared (FTIR), ^1H nuclear magnetic resonance (NMR), electronic spectra, scanning electron micrography (SEM), N_2 adsorption-desorption isotherm, and dynamic light scattering (DLS) studies. In this paper, we present our results and propose possible structures for synthesized compounds based on several spectral data. The unique nature of the work presented is the porosity of compounds which has been explored here.

Results and discussion

Elemental analysis and solubility

The compounds are fully soluble in dimethyl sulfoxide (DMSO) but partially soluble in ethanol. The compounds are insoluble in other solvents.

PXRD analysis

The compounds were examined for crystalline/amorphous nature by PXRD in as obtained state. All the compounds are assumed to be isostructural on the basis of their powder X-ray diffraction diagrams (Figure 1). Further, all the compounds produce highly intense X-ray reflections in their corresponding PXRD pattern, indicating that all the compounds are crystalline in nature. The broadness of the diffraction peaks indicates that the particles are of nanometer dimensions. The average crystallite size of the nanoparticles was calculated using Scherrer's formula:

$$L = 0.89\lambda / \beta \cos\theta,$$

where L is the average crystallite size, λ = 1.5418Å for CuKα, β is the half maximum peak width, and θ is the diffraction angle in degrees. The average crystallite size has been found to be about 40 nm.

Figure 1 PXRD patterns for (a) 1, (b) 2, and (c) 3.

FTIR spectral data

In PPD, two sharp bands observed at 3,498 and 3,450 cm^{-1} are due to ν_{as}(N-H) and ν_{s}(N-H) stretching modes of NH_2 group (Figure 2). In compounds **1**, **2**, and **3**, these bands appear at 3,463 and 3,420 cm^{-1}, respectively (Figure 3), confirming the presence of primary aromatic amine (NH_2) group [21]. A strong band near 1,605 cm^{-1} is due to N-H bending mode of NH_2 group [22]. A weaker absorption band near 3,203 cm^{-1} is the Fermi resonance band which appeared as a result of the interaction between the overtone of the 1,605 cm^{-1} band with the symmetric N-H stretching band. Further, bands at 1,276, 3,038, 835, and 1,502 cm^{-1} are assigned as C-N aromatic stretching [23], C-H aromatic stretching, C-H aromatic deformation [22,23], and C=C aromatic stretching bands [22], respectively. The new non-ligand bands observed in the region around 605 and 420 cm^{-1} are assigned to the υ(M–N) bands and υ(M–O) bands, respectively [24]. The broad band around 3,200 cm^{-1} is due to υ(OH) of coordinated water molecules [24-27].

Figure 2 FTIR spectrum of PPD.

Figure 3 FTIR spectra of (a) 1, (b) 2, and (c) 3.

^{1}H NMR study

The ^{1}H NMR spectra of PPD and compound **1** were recorded in deuterated DMSO. The ^{1}H NMR spectrum of PPD showed two signals (Figure 4a). The sharp signal at δ 6.31 is due to

aromatic protons, whereas the broad signal at δ 3.37 is due to protons of -NH_2 group. The peak at δ 2.50 is the residual solvent peak.

Figure 4 ^{1}H NMR spectra of (a) PPD and (b) 1.

The ^{1}H NMR spectrum of **1** (Figure 4b) is also characterized by the two signals which exactly correspond to two types of protons in **1**. Compared to the spectrum of PPD, broad signal at δ 4.00 in the spectrum of **1** is attributed to the -NH_2 protons of the benzenoid ring, whereas the aromatic protons of the benzenoid ring appear as a sharp signal at δ 6.50. Again, the peak at δ 2.50 is the residual solvent peak.

UV–vis spectral studies

The UV–vis spectra of PPD and compounds **1**, **2,** and **3** were recorded in dimethyl sulfoxide to investigate their electronic properties. The UV–vis spectrum of PPD (Figure 5) shows three narrow and intense characteristic absorption bands centered at 199, 237, and 299 nm. The bands located at 199 and 237 nm can be assigned to π-π* transitions of the benzenoid rings, whereas the weak band centered at 299 nm is ascribed to the transition derived from a so-called π-p conjugation by the unshared electrons of NH_2 and benzenoid ring [28,29]. However, in **1**, **2,** and **3** (Figure 6), the bands due to the π-π* transitions undergo bathochromic shift to 246 nm, and the band due to the π-p transition undergoes bathochromic shift to 338 nm when compared with the spectrum of PPD. It is probable that bathochromic shift occurs as a result of the coordination of the lone pair electrons on the N donor atoms of PPD with the metal ion site, thus stabilizing the excited state relative to the ground state, leading to longer wavelength absorption maxima [30].

Figure 5 UV–vis spectrum of PPD.

Figure 6 UV–vis spectrum of (a) 1, (b) 2, and (c) 3.

Magnetic studies

The observed magnetic moment values of **1** and **2** at room temperature are 1.71 and 2.80 BM, respectively, suggesting their paramagnetic nature, whereas compound **3** was found diamagnetic in nature. The values correspond to +2 oxidation state for Cu, Ni, and Zn in the respective compounds.

Morphology and dynamic light scattering DLS studies

The morphologies of **1**, **2,** and **3** were determined by SEM. Typical SEM images of the particles of **1**, **2,** and **3** are shown in Figures 7, 8, and 9, respectively. As depicted from low magnification SEM images, only a few particles are in single state, while most of the particles are prone to condense with each other and form nanoclusters. Higher magnification SEM images reveal that these nanoclusters form a porous network structure.

Figure 7 Typical SEM images of the particles of 1. (**a**) Low magnification SEM image, (**b**) and (**c**) high magnification SEM images.

Figure 8 Typical SEM images of the particles of 2. (**a**) Low magnification SEM image, (**b**) and (**c**) high magnification SEM images.

Figure 9 Typical SEM images of the particles of 3. (**a**) Low magnification SEM image, (**b**) and (**c**) high magnification SEM images.

We further examined the particle size of each compound by DLS technique. All the compounds were dispersed in water by sonication for 5 min. As observed from Figure 10, the DLS measurements show mean particle sizes of 400, 340, and 360 nm for **1**, **2**, and **3** respectively, with narrow size distribution.

Figure 10 Particle size measurement of (a) 1, (b) 2 and (c) 3 in water by DLS technique.

N_2 adsorption-desorption isotherm: textural/structural properties

Figure 11a shows the nitrogen sorption isotherm of **1**. The figure suggests that according to IUPAC classification, compound **1** exhibits type IV reversible isotherm with *H1* hysterisis, characteristic of mesoporous materials. The inflection occurs at relative pressure 0.09. Generally, the inflection position depends on the diameter of mesopores, and sharpness usually indicates the uniformity of the mesopores. The higher the value of inflection position, the bigger the diameter of mesopores. The greater the sharpness, the more uniformity the mesopores are. The inflection position corresponds to the pronounced uptake of nitrogen and indicates the stage at which the monolayer coverage is complete and the multilayer adsorption is about to begin.

Figure 11 Surface area and porosity studies of 1. (**a**) N_2 sorption isotherm, (**b**) BET plot, (**c**) *t*-plot analysis, and (**d**) BJH pore size distribution As observed from the isotherm, compound **1** shows steep adsorption. This indicates that compound **1** possesses mesopores of uniform order and has ordered structural as well as textural features [31]. In addition, the hysteresis loop observed at higher relative pressure indicates that it possesses large pores [32] which are filled at relatively higher pressures by capillary condensation of N_2. The type *H1* further suggests that the polymer consists of *agglomerates* [33].

The specific surface area determined by Brunauer-Emmett-Teller (BET) method is found to be 65.25 m^2/g (Figure 11b), whereas the Langmuir surface area is found to be 87.3 m^2/g. The values of the micropore volume, micropore area, and external surface area obtained by the *t*-method micropore analysis (de Boer) are 0.00012 cc/g, 0.35 m^2/g, and 64.9 m^2/g, respectively (Figure 11c). Thus, total BET surface area (65.25 m^2/g) is exactly equal to the sum of the micropore area (0.35 m^2/g) and external the surface area (64.9 m^2/g). This behavior further confirms that compound **1** satisfies the BET analysis with type IV isotherm, indicating the formation of multiple layers during adsorption [33]. The surface area of the micropores is relatively low compared with the other porous crystalline structures, which might be caused by the relatively compact structure of the polymer [34].

In view of further verification, the pore size distribution pattern was obtained from the desorption branch by employing Barrett-Joyner-Halenda (BJH) model and is illustrated in Figure 11d. The distribution curve shows that the pores present in the polymer are of variable sizes with their diameters ranging from 1.4 to 12.4 nm. The maxima of the curve occurs at 2.3 nm, suggesting that majority of the pores have diameters of 2.3 nm. The average pore

diameter was found to be 5.2 nm, whereas the total pore volume has been found to be 0.085 cc/g for pores smaller than 19 nm diameter at relative pressure *P*/*P*o = 0.89.

Proposed mechanism of polymerization

A plausible formation process is briefly presented as following:

While preparing aqueous solutions of the respective metal salts, M^{2+} ions get hydrated and form hexa-aqua complexes. When these aqua complexes are mixed with aqueous solution of PPD, two water molecules on the trans positions of aqua complex are replaced by two PPD molecules, resulting in tetra-aqua PPD substituted complex. The free nitrogen atoms of the coordinated PPD can further capture hexa-aqua complex molecules by coordination interactions. This coordination-induced assembly process can proceed repeatedly until the depletion of reactants in the solution, resulting in the formation of large coordination polymers having a porous structure. The Cl^- anions are accommodated in this porous structure as the counter ions. Thus, we get one-dimensional linear coordination polymers comprising a repeat unit shown in Scheme 1 in which the *M*(II) ion is six- coordinated. The *M*(II) ion binds to four oxygen atoms from the four coordinated water molecules (which come from aqueous medium) and two nitrogen atoms from two different PPD ligands in the distorted octahedral coordination geometry. However, the detailed formation mechanism of such coordination polymers is not clear at present time and needs further investigation. However, the proposed mechanism is shown as Scheme 2.

Scheme 1 One-dimensional linear coordination polymers comprising a repeat unit.

Scheme 2 Proposed mechanism.

Conclusions

Mesoporous nanostructured metal-organic hybrid materials composed of copper(II), nickel(II), and zinc(II) metal ions with PPD as the organic ligand were synthesized at room temperature. The proposed formula of the compounds is $\{[M(H_2O)_4(PPD)_2]^{2+}.2Cl^-\}_n$, where *M* = Cu, Ni or Zn. The PXRD profile shows the crystalline nature of the polymers. N_2 adsorption-desorption isotherm confirms the mesoporous nature of **1** as it exhibits type IV isotherm with *H1* hysterisis. The steepness of the inflection point shows that the mesopores formed are of uniform order. The BJH curve shows an average pore diameter of 5.2 nm. The specific surface area determined by the BET method is 65.25 m^2/g.

Methods

Materials

Doubly-distilled water was used to prepare aqueous solutions. *p*-Phenylenediamine was received from Sigma-Aldrich (MO, USA). $CuCl_2$, $NiCl_2.6H_2O$, and $ZnCl_2$ were of analytical grade and used without further purification.

Characterization techniques

Microanalyses were carried out using CHNS analyzer Leco Model-932 (LECO Corporation, St. Joseph, MI, USA). The concentrations of the metal ions were estimated by atomic absorption spectroscopy (Perkin-Elmer2380, Waltham, MA, USA). PXRD patterns were recorded from 0° to 70° on a Rigaku Miniflex diffractometer using monochromatic CuKα radiations (The Woodlands, TX, USA). FTIR spectra from 4,000 to 400 cm^{-1} were recorded on Perkin-Elmer Spectrum RX 1 FTIR spectrophotometer using KBr disks. ^1H NMR spectra were recorded on Bruker Avance DPX 200 NMR spectrometer (200 MHz; Dubai, UAE) using tetramethyl silane as internal standard. Electronic spectra (190 to 800 nm) of 10^{-3} M ethanolic solutions of PPD and its compounds with Ni(II), Cu(II), and Zn(II) were recorded on UV-visible double beam spectrophotometer, PG Instruments Ltd. Model T90+ (Leicestershire, England). Scanning electron micrographs (SEM) were collected on Jeol T-300 scanning electron microscope with gold coating (Tokyo, Japan). The particle size of each compound was determined by DLS technique using Zetasizer Nano ZS-90 (Malvern Instruments Ltd., Worcestershire, UK.

N_2 adsorption-desorption and Brunauer-Emmett-Teller surface area studies

The specific surface area, total pore volume, and average pore diameter were measured by N_2 adsorption-desorption method using NOVA 1200 (Quanta Chrome, Boynton Beach, FL, USA) instrument. The bath temperature was maintained at 77 K. The sample was degassed at 423 K for 12 h before measurement. Pore size distribution and pore volume were obtained by applying BJH analysis to the adsorption branch of the nitrogen adsorption-desorption isotherm. The specific surface area of the sample was calculated using Brunauer-Emmett-Teller method. Micropore surface area and micropore volume were determined from *t*-plot analysis. All the flow rates were maintained at normal temperature and pressure.

Synthesis of *M*(II)-PPD compounds (*M*(II) = Cu(II), Ni(II), Zn(II))

In a typical experiment, 1.4 ml of 15 M PPD aqueous solution was introduced into 40 ml of water first, and then 5.5 ml of 3.8 M aqueous solution of the metal salt; $CuCl_2$/$NiCl_2.6H_2O$/$ZnCl_2$ with 1:1 molar ratio of PPD to metal was added into the resulting solution under vigorous stirring at room temperature. A gradual color change was observed, and a large amount of blackish-brown-colored precipitates occurred within several hours. The precipitates thus formed were collected by centrifugation, washed several times with absolute ethanol and water, and then dried in air. The yield percentage obtained in each case was around 68%.

- Elemental analysis of the compound composed of Cu(II) with PPD, **1**: ($C_{12}H_{24}CuN_4O_4$, 351.89): Calc: C 40.96, H 6.87, N 15.92, Cu 18.06%; Found: C 40.85, H 6.75, N 15.78, Cu 18.25%.
- Elemental analysis of the compound composed of Ni(II) with PPD, **2**: ($C_{12}H_{24}NiN_4O_4$, 347.04): Calc: C 41.53, H 6.97, N 16.14, Ni 16.91%; Found: C 41.69, H 6.66, N 16.78, Ni 16.55%.
- Elemental analysis of the compound composed of Zn(II) with PPD, **3**: ($C_{12}H_{24}ZnN_4O_4$, 353.73): Calc: C 40.74, H 6.84, N 15.84, Zn 18.49%; Found: C 40.85, H 6.65, N 15.68, Zn 18.25%.

Competing interests

The authors declare that they have no competing interest.

Authors' contributions

RG, SS, HNS, and BLK provided the same contributions in this article. All authors read and approved the final manuscript.

Authors' information

RG was born in Jammu, India. She received her M.Sc. degree in Chemistry from the University of Jammu in 2008 and M. Phil. degree in Chemistry from the same university in 2009 under the supervision of Dr. Sheikh. Presently, she is doing her Ph.D. study in Chemistry from the same university, under the supervision of Dr. Sheikh. SS was born in Jammu, India. He received his M.Sc. degree in Chemistry from the University of Jammu in 2009. Presently, he is doing his Ph.D. study in Chemistry from the same university under the supervision of Dr. Sheikh. HNS was born in Jammu, India. He received his M.Sc. degree in Chemistry from the University of Jammu in 1992, and Ph.D. degree in Chemistry from the same university in 1998. He joined the Department of Chemistry, University of Jammu as Lecturer in 1999, became Associate Professor in 2006, and Professor in 2013. He is presently working as Professor in the Department of Chemistry, University of Jammu, Jammu. At present, he is actively involved in research in coordination polymers and nanomaterials, and has M. Phil. and Ph.D. students in these fields. BLK was born in Jammu, India. He received his M.Sc. degree in Chemistry from J & K University 1969, Ph. D. degree in Chemistry from Delhi University in 1973, and Post Doctoral degree from UTEP, El Paso, Texas, USA in 1978. He retired as Dean of the Faculty of Science, University of Jammu in 2007. He has worked on much scientific research areas such as Organometallic Chemistry, Coordination Chemistry, Environmental Chemistry, and Nanomaterials.

Acknowledgments

The authors gratefully acknowledge the financial support from the Defence Research Development Organization, New Delhi. They thank the Department of Anatomy, All India Institute of Medical Sciences, New Delhi for the Electron Microscope Facility. They are also thankful to the National Chemical Laboratory, Pune for the thermal, powder X-ray diffraction, and adsorption-desorption studies.

References

1. James, SL: Metal-organic frameworks. Chem. Soc. Rev. **32**, 276–288 (2003)

2. Eddaoudi, M, Moler, DB, Li, H, Chen, B, Reineke, MR, O'Keeffe, M, Yaghi, O: Modular chemistry: secondary building units as a basis for the design of highly porous and robust metal-organic carboxylate frameworks. Accounts Chem. Res. **34**, 319–330 (2001)

3. Seo, JS, Whang, D, Lee, H, Jun, SI, Oh, J, Jeon, YJ, Kim, K: A homochiral metal-organic porous material for enantioselective separation and catalysis. Nature **404**, 982–986 (2000)

4. Fukuoka, A, Sakamoto, Y, Guan, S, Inagaki, S, Sugimoto, N, Yukushima, F, Hirahara, K, Iijima, S, Ichikawa, MJ: Novel templating synthesis of necklace-shaped mono-and bimetallic nanowires in hybrid organic–inorganic mesoporous material. J. Am. Chem. Soc. **123**, 3373–3374 (2001)

5. Shi, H, Qi, L, Ma, L, Cheng, H: Polymer-directed synthesis of penniform $BaWO_4$ nanostructures in reverse micelles. J. Am. Chem. Soc. **125**, 3450–3451 (2003)

6. Zhang, H, Yang, D, Li, D, Ma, X, Li, S, Que, D: Controllable growth of ZnO microcrystals by a capping-molecule-assisted hydrothermal process. Cryst. Growth Des. **5**, 547–550 (2005)

7. Kuang, D, Xu, A, Fang, Y, Liu, H, Frommen, C, Fenske, D: Surfactant-assisted growth of novel PbS dendritic nanostructures via facile hydrothermal process. Adv. Mater. **15**, 1747–1750 (2003)

8. Kim, F, Connor, S, Song, H, Kuykendall, T, Yang, P: Platonic gold nanocrystals. Angew. Chem. Int. Ed. **43**, 3673–3677 (2004)

9. Markovich, G, Collier, CP, Henrichs, SE, Remacle, F, Levine, RD, Heath, JR: Architectonic quantum dot solids. Acc. Chem. Res. **32**, 415–423 (1999)

10. Lin, W, Rieter, J, Taylor, KML: Modular synthesis of functional nanoscale coordination polymers. Angew. Chem. Int. Ed Engl. **48**(4), 650–658 (2009)

11. Taylor, KML, Rieter, WJ, Lin, W: Manganese-based nanoscale metal-organic frameworks for magnetic resonance imaging. J. Am. Chem. Soc. **130**, 14358–14359 (2008)

12. Rieter, WJ, Pott, KM, Taylor, KML, Lin, W: Nanoscale coordination polymers for platinum-based anticancer drug delivery. J. Am. Chem. Soc. **130**, 11584–11585 (2008)

13. Sahraneshin, A, Asahina, S, Togashi, T, Singh, V, Takami, S, Hojo, D, Arita, T, Minami, K, Adschiri, T: Surfactant-assisted hydrothermal synthesis of water-dispersible hafnium oxide nanoparticles in highly alkaline media. Cryst. Growth Des. **12**(11), 5219–5226 (2012)

14. Tsuroka, T, Kawasaki, H, Nawafune, H, Akamatsu, K: Controlled self-assembly of metal–organic frameworks on metal nanoparticles for efficient synthesis of hybrid nanostructures. Appl. Mater. Interfaces. **3**(10), 3788–3791 (2011)

15. Bourne, SA, Mangombo, Z: Phenylamines as building blocks to layered inorganic–organic structures. Cryst. Eng. Comm. **6**, 437–442 (2004)

16. Pansanel, J, Jouaiti, A, Ferlay, S, Hosseini, M: Molecular tectonics: generation of 2-D molecular networks by combination of coordination and hydrogen bonds. New J. Chem. **30**, 71–76 (2006)

17. Sun, X, Dong, S, Wang, E: Coordination-induced formation of submicrometer-scale, monodisperse, spherical colloids of organic–inorganic hybrid materials at room temperature. J. Am. Chem. Soc. **127**, 13102–13103 (2005)

18. Mederos, A, Dominguez, S, Hernandez-Molina, R, Sanchiz, J, Brito, F: Coordinating ability of phenylenediamines. Coord. Chem. Rev. **193–195**, 913–939 (1999)

19. Mederos, A, Dominguez, S, Hernandez-Molina, R, Sanchiz, J, Brito, F: Coordinating ability of ligands derived from phenylenediamines. Coord. Chem. Rev. **193–195**, 857–911 (1999)

20. Han, MG, Foulger, SH: Crystalline colloidal arrays composed of poly(3,4-ethylenedioxythiophene)-coated polystyrene particles with a stop band in the visible regime. Adv. Mater. **16**(3), 231–234 (2004)

21. Wang, JJ, Jiang, J, Hu, B, Yu, SH: Uniformly shaped poly(*p*-phenylenediamine) microparticles: shape-controlled synthesis and their potential application for the removal of lead ions from water. Adv. Funct. Mater. **18**(7), 1105–1111 (2008)

22. Cataldo, F: On the polymerization of *p*-phenylenediamine. Eur. Polym. J. **32**(1), 43–50 (1996)

23. Mallick, K, Witcomb, MJ, Dinsmore, A, Scurrell, MS: Fabrication of metal nanoparticles and polymer nanofibers composite material by an in situ chemical synthetic route. Langmuir **21**(17), 7964–7967 (2005)

24. Nakamoto, K: Infrared and Raman Spectra of Inorganic and Coordination Compounds, 5th edn. Wiley, New York (1997)

25. Ding, B, Liu, YY, Zhao, XJ, Yang, EC, Wang, XG: Hydrothermal synthesis and characterization of a novel luminescent lead(II) framework extended by novel Pb-μ1,1-(N)CS-Pb bridges. J. Mol. Struct. **920**, 248–251 (2009)

26. Luo, Y-M, Li, J, Xiao, L-X, Tang, R-R, Tang, X-C: Synthesis, characterization and fluorescence properties of Eu(III) and Tb(III) complexes with novel mono-substituted-diketone ligands and 1,10-phenanthroline. Spectrochim. Acta Part A. **72**, 703–708 (2009)

27. Xie, C, Zhang, Z, Wang, X, Liu, X, Shen, G, Wang, R, Shen, D: The synthesis and structure of a novel 1D copper(II) weak coordination polymer with 2,6-pyridinedicarboxylic acid. J. Coord. Chem. **57**, 1173–1178 (2004)

28. Min, Y-L, Wang, T, Zhang, Y-G, Chen, Y-C: The synthesis of poly(*p*-phenylenediamine) microstructures without oxidant and their effective adsorption of lead ions. J. Mater. Chem. **21**, 6683–6689 (2011)

29. Liu, Z, Zu, Y, Fu, Y, Guo, S, Zhang, Y, Liang, H: Synthesis of hybrid nanostructures composed of copper ions and poly(*p*-phenylenediamine) in aqueous solutions. J. Nanopart. Res **10**(8), 1271–1278 (2008)

30. Christie, RM: Colour Chemistry, pp. 12–44. Royal Society of Chemistry, United Kingdom (2001)

31. Jha, RK, Shylesh, S, Bhoware, SS, Singh, AP: Oxidation of ethyl benzene and diphenyl methane over ordered mesoporous M-MCM-41 (M = Ti, V, Cr): synthesis, characterization and structure–activity correlations. Micropor. Mesopor. Mater **95**(1–3), 154–163 (2006)

32. Shylesh, S, Jha, RK, Singh, AP: Assembly of hydrothermally stable ethane-bridged periodic mesoporous organosilicas with spherical and wormlike structures. Micropor. Mesopor. Mater. **94**(1–3), 364–370 (2006)

33. Sing, KSW, Everett, DH, Haul, RAW, Moscou, L, Pierotti, RA, Rouquerol, J, Siemieniewska, T: Reporting physisorption data for gas/solid systems with special reference to the determination of surface area and porosity. Pure Appl. Chem. **57**, 603–619 (1985)

34. Huo, J, Wang, L, Irran, E, Yu, H, Gao, J, Fan, D, Li, B, Wang, J, Ding, W, Amin, AM, Li, C, Ma, L: Hollow ferrocenyl coordination polymer microspheres with micropores in shells prepared by Ostwald ripening. Angew. Chem. **49**(48), 9237–9241 (2010)

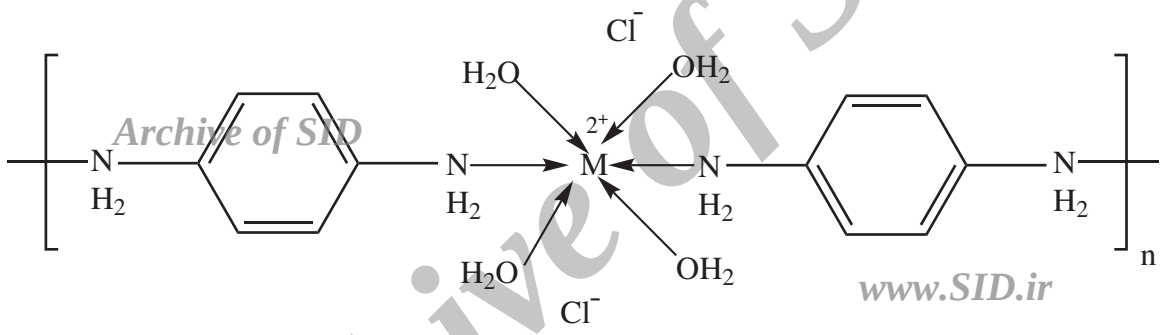

Scheme 1

M = Cu, Zn or Ni

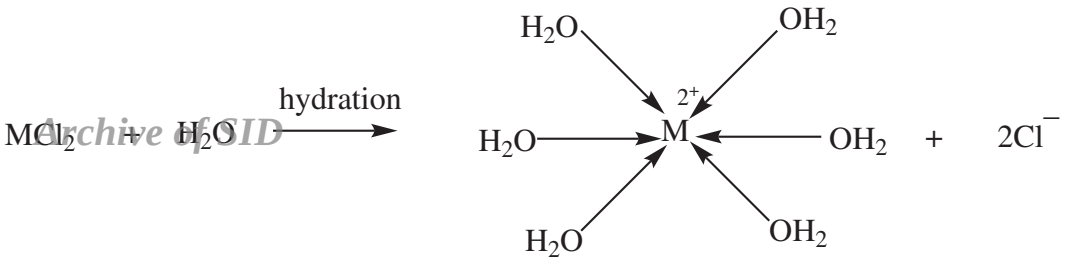

Aqua complex

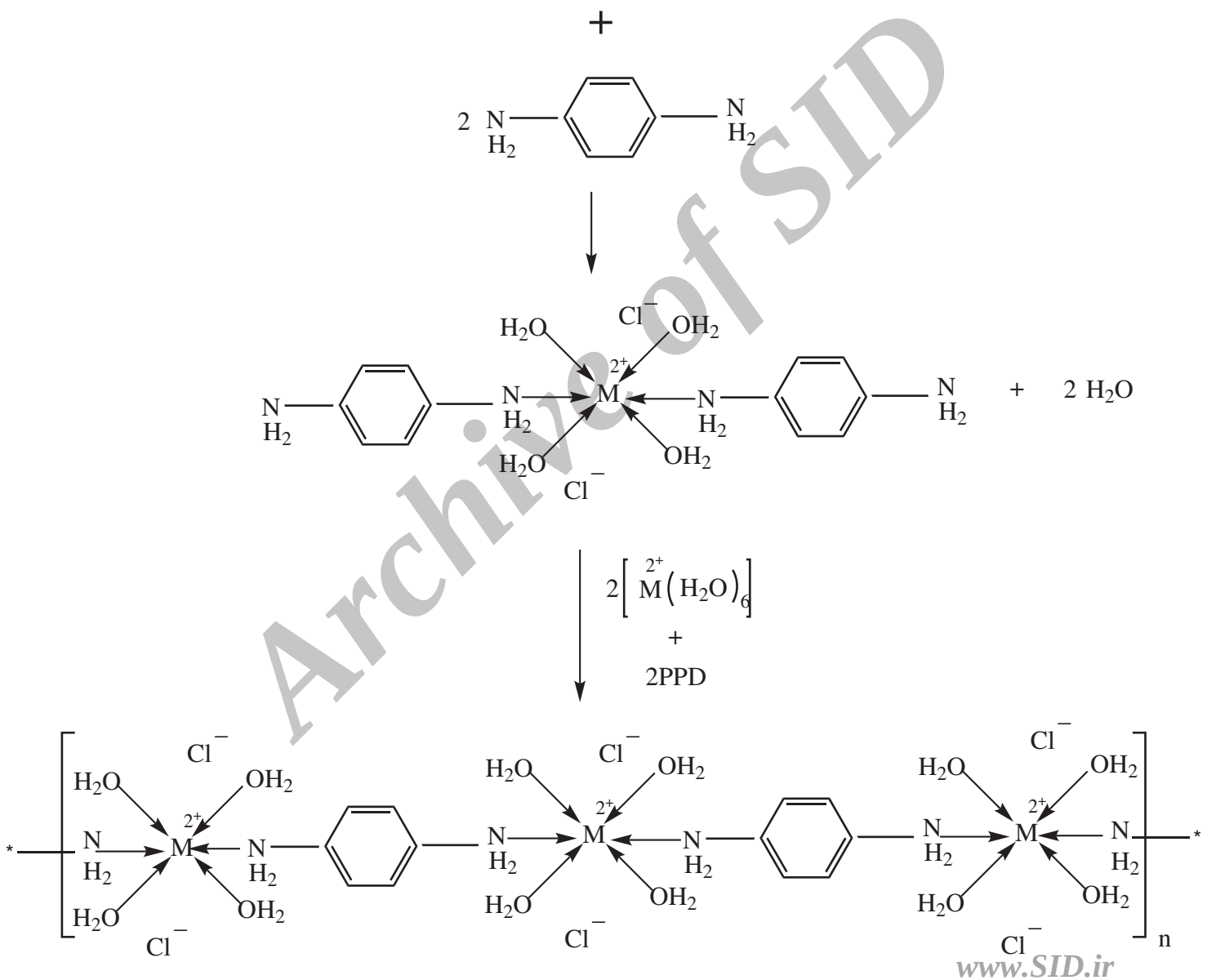

Scheme 2

M = Cu, Ni or Zn

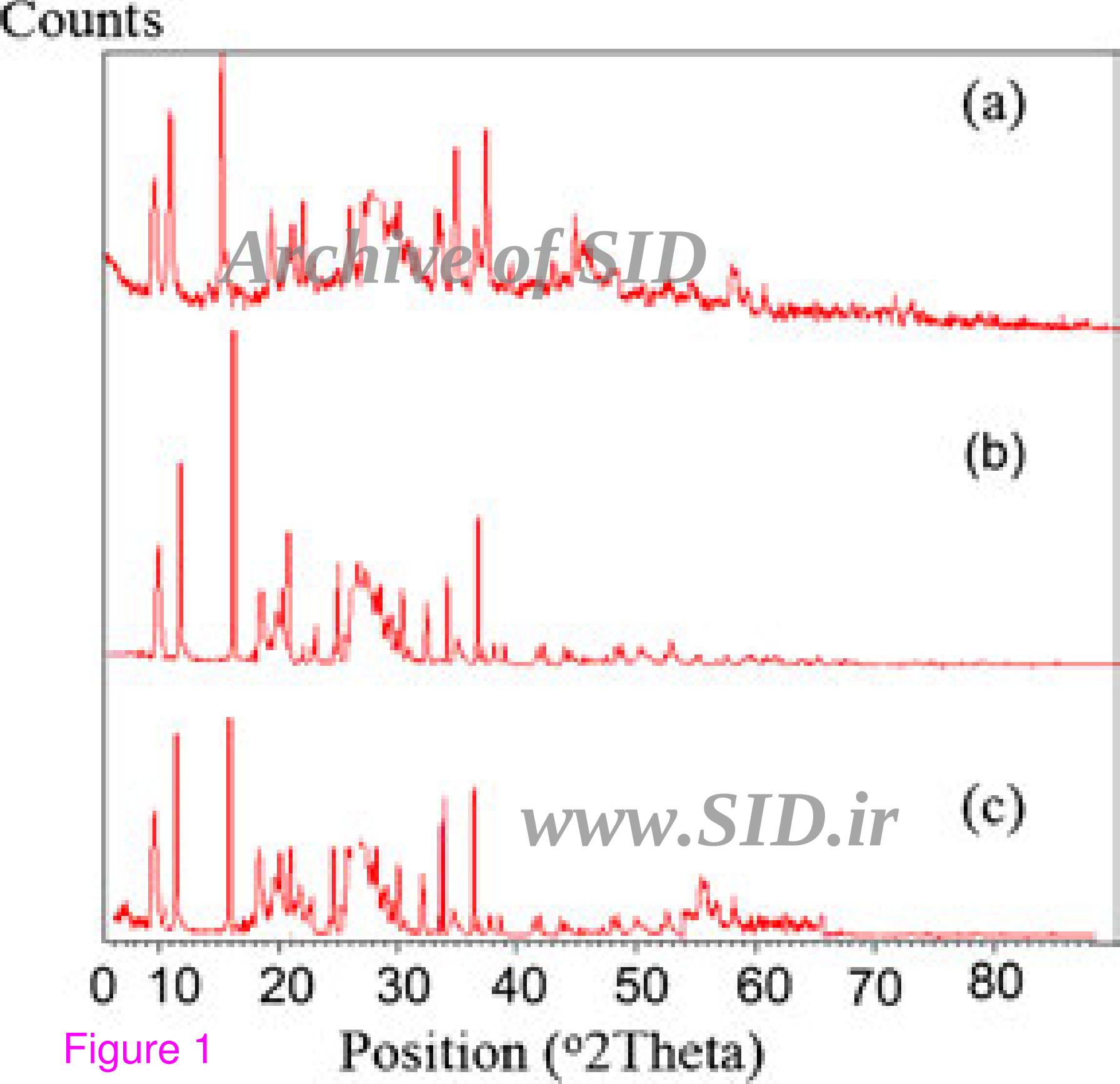

Figure 1

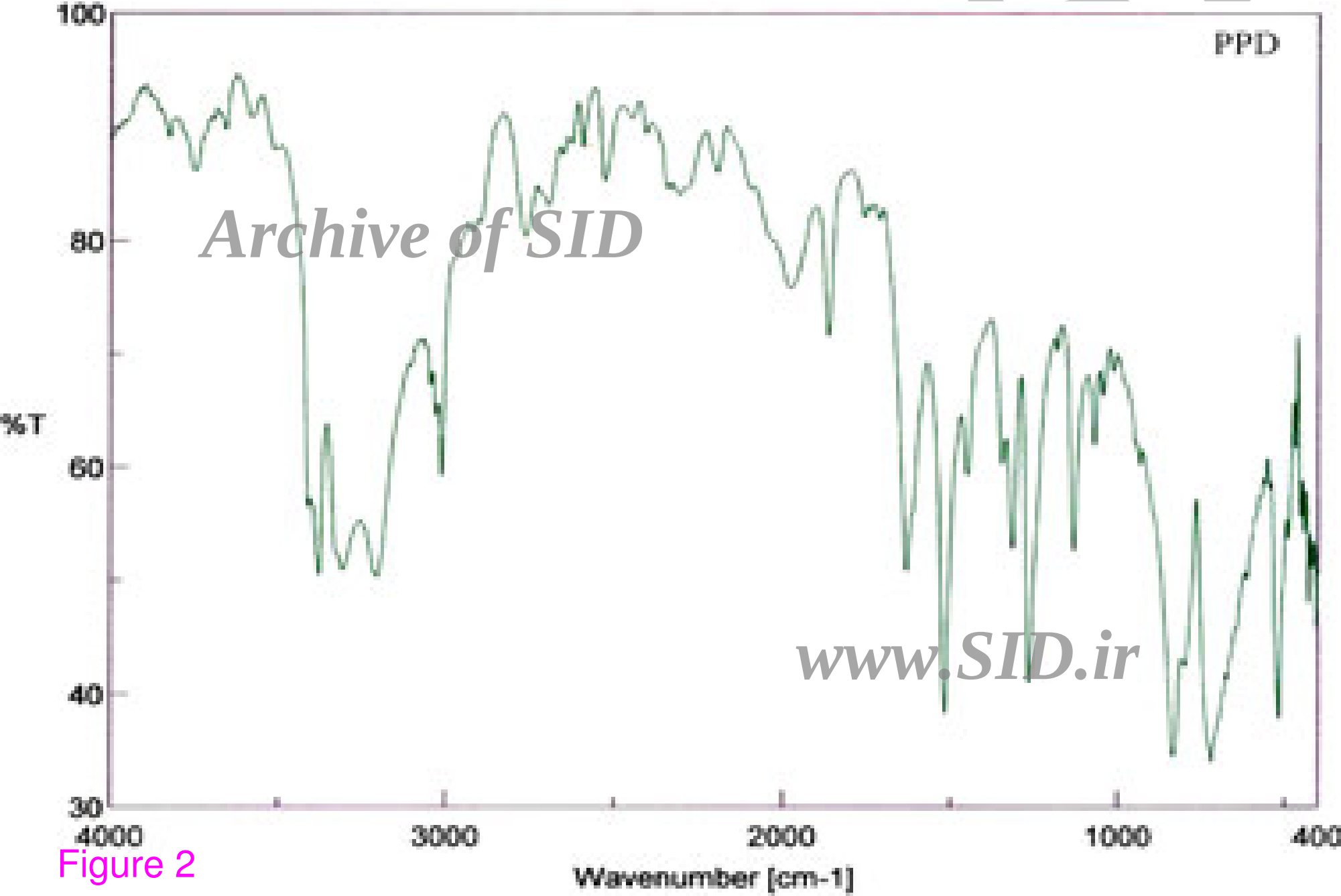

Figure 2

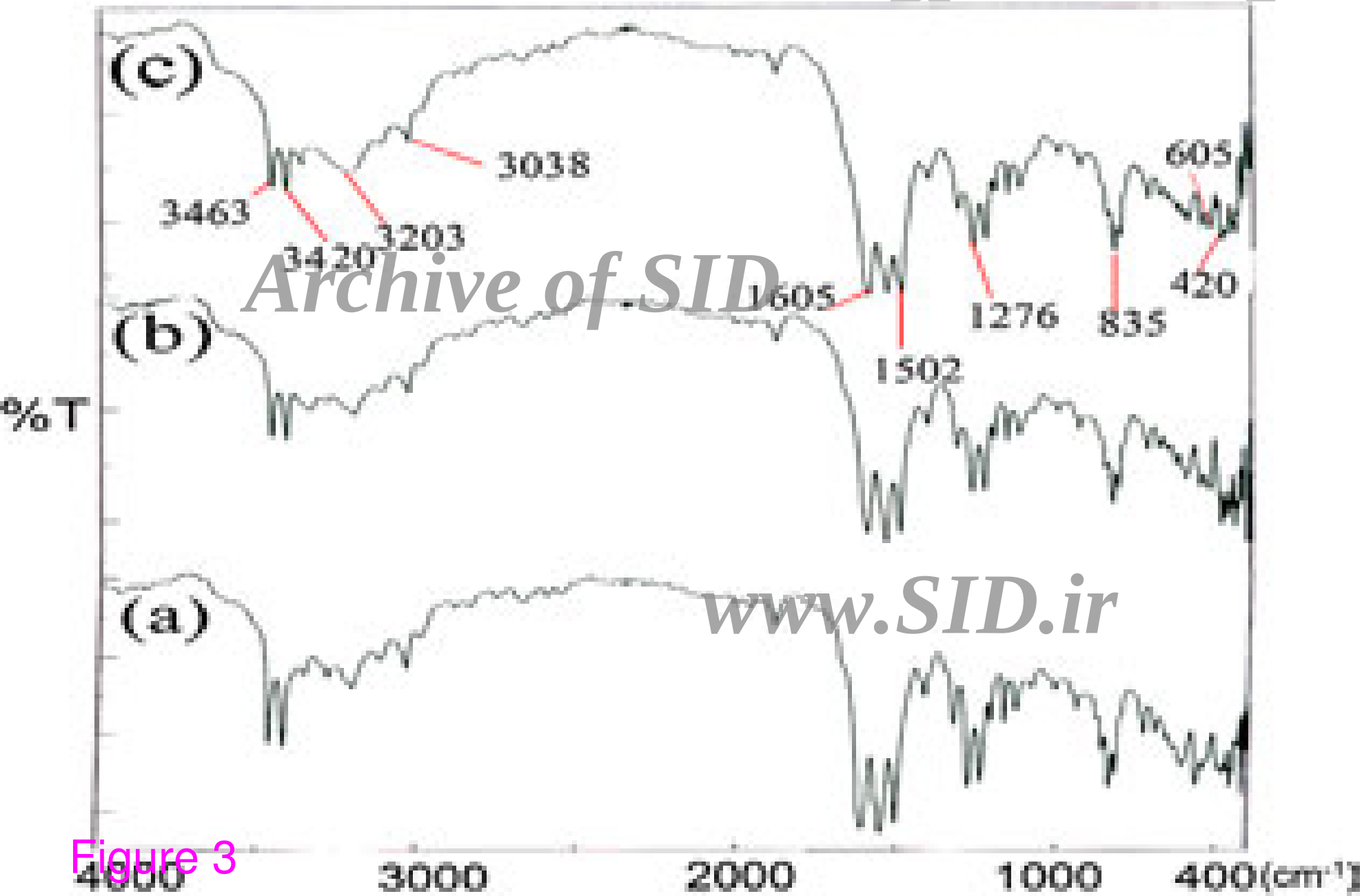

Figure 3

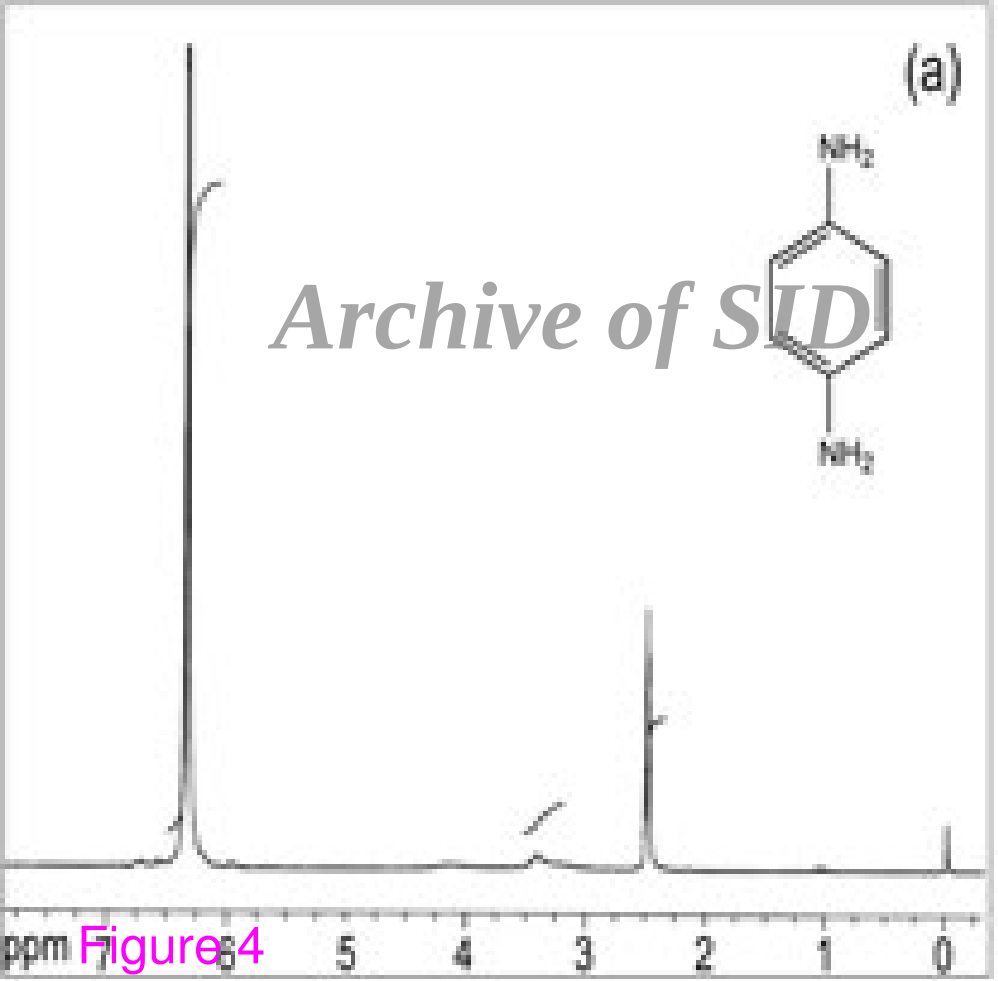

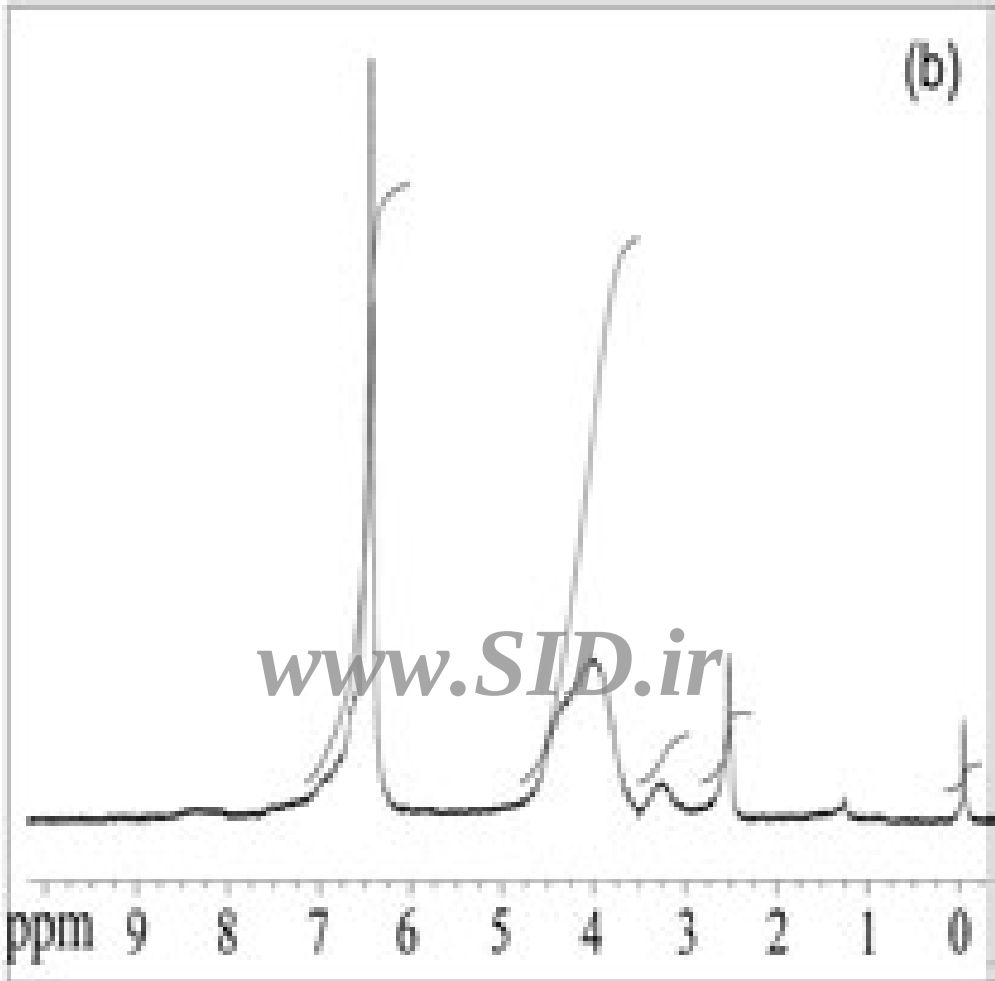

Figure 4

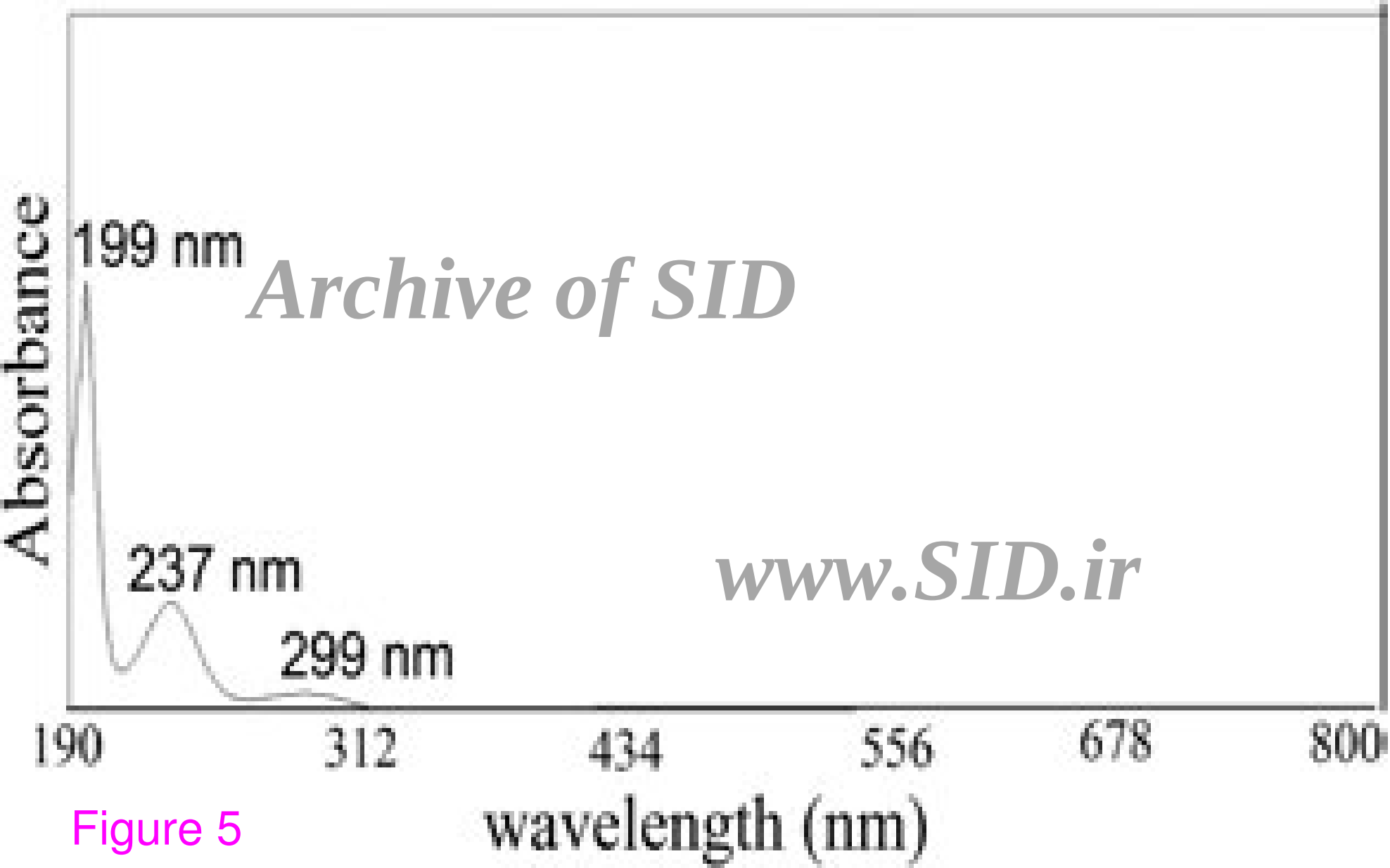

Figure 5

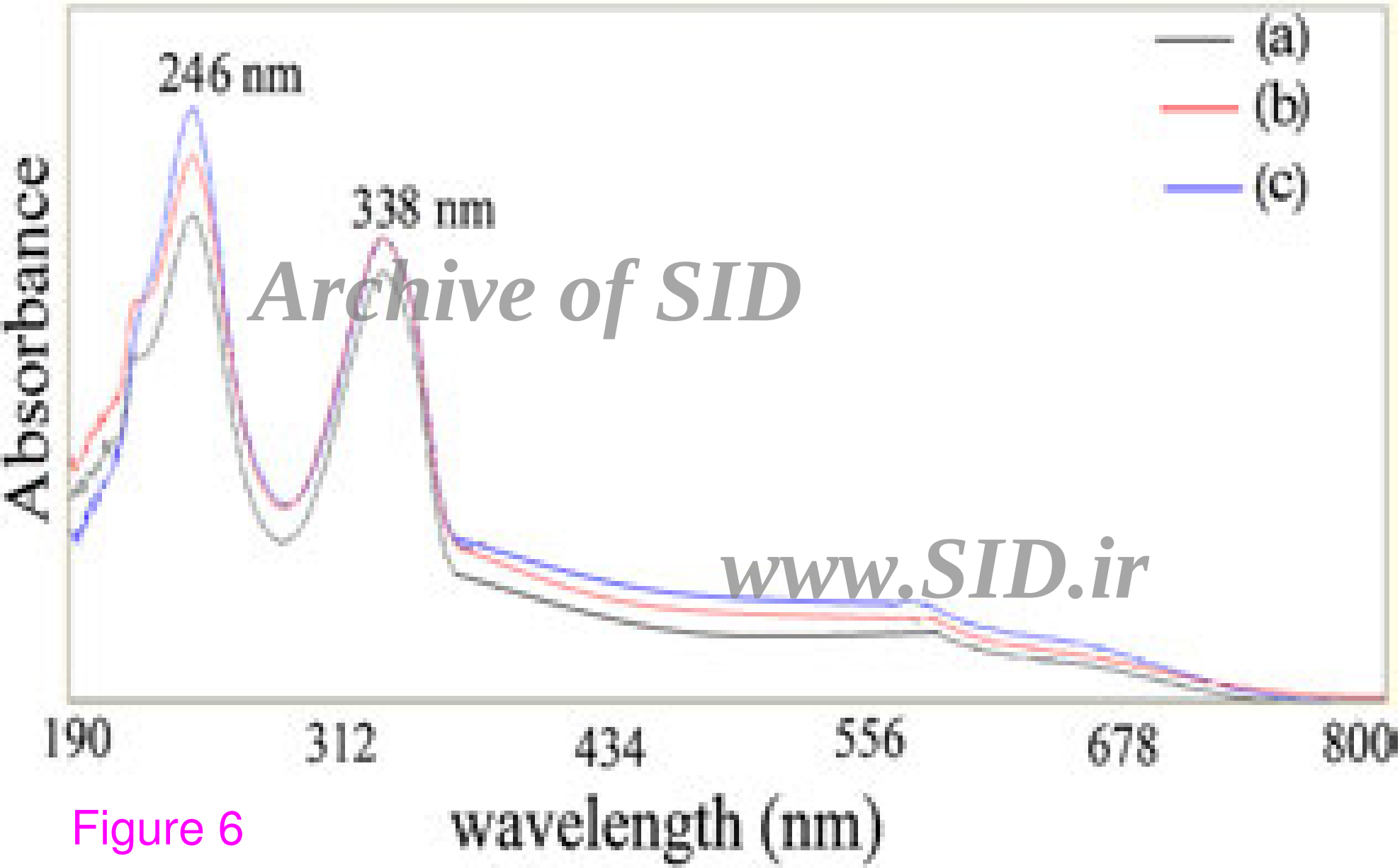

Figure 6

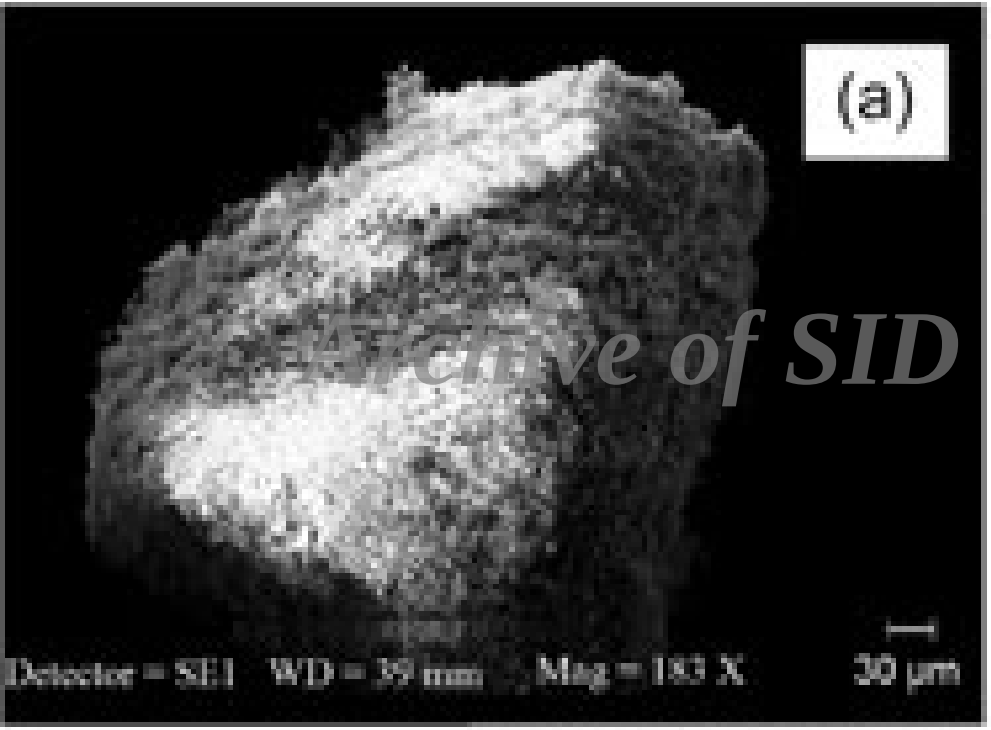

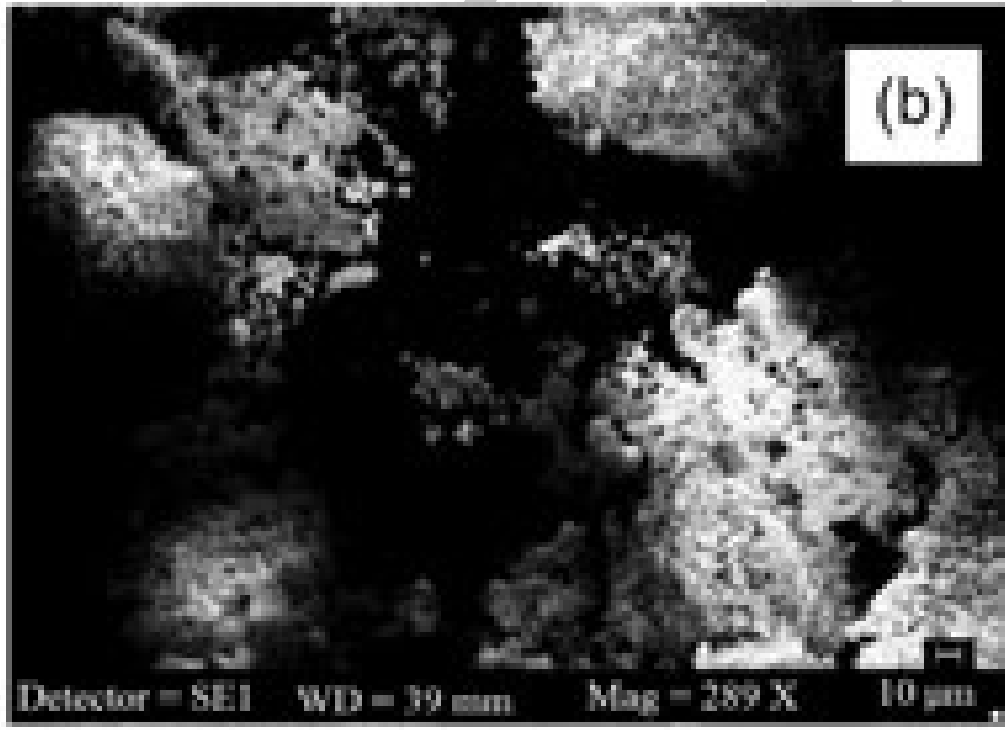

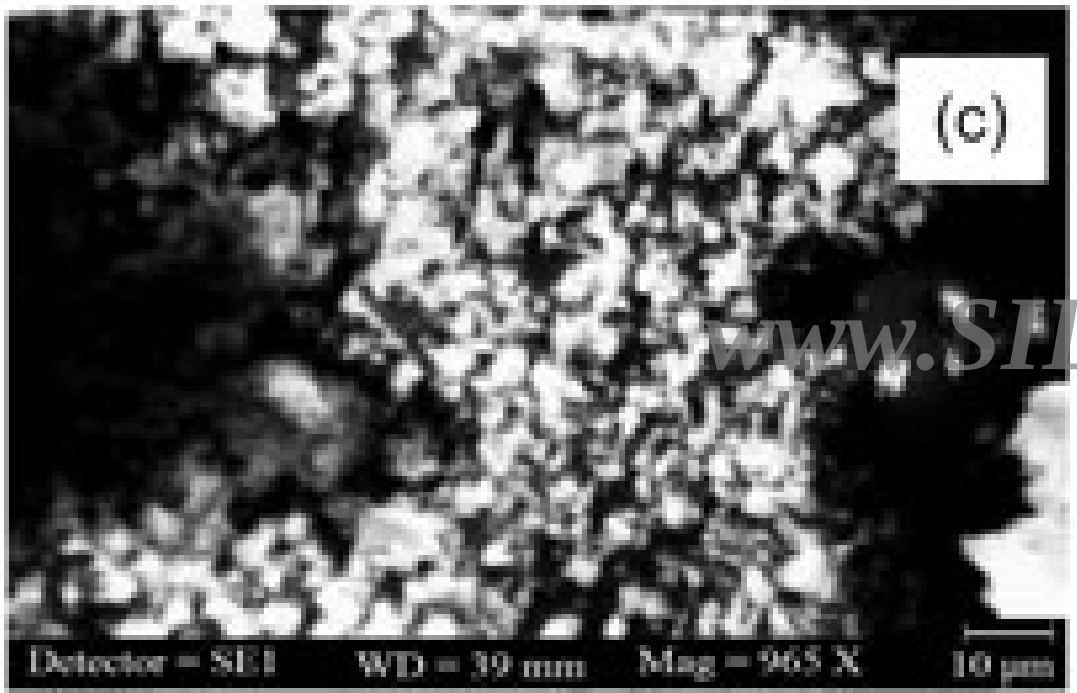

Figure 7

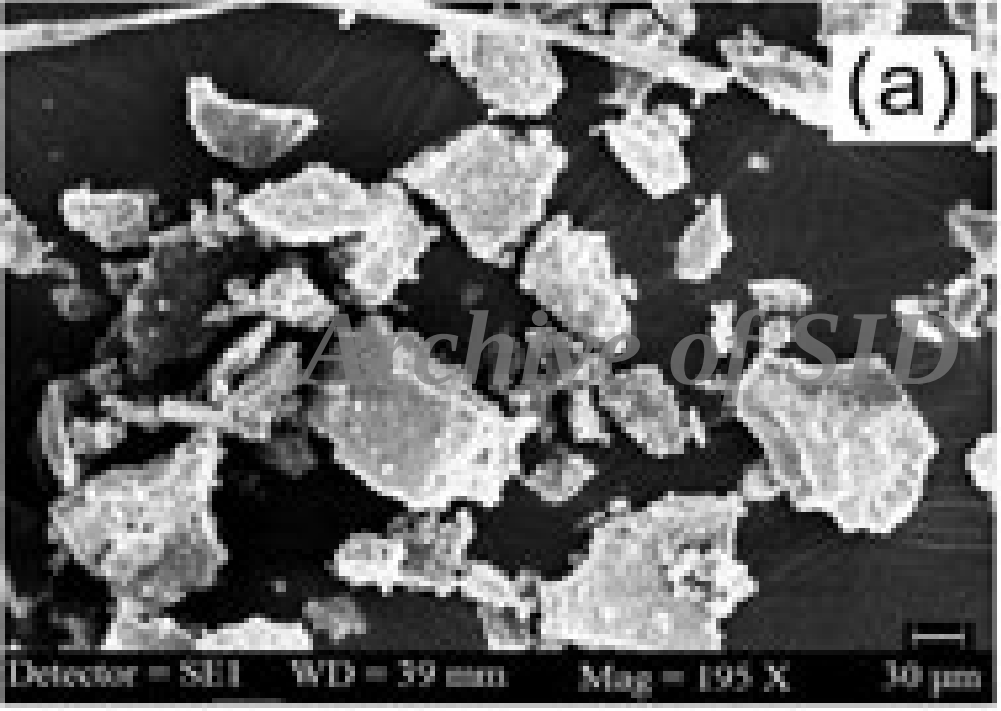

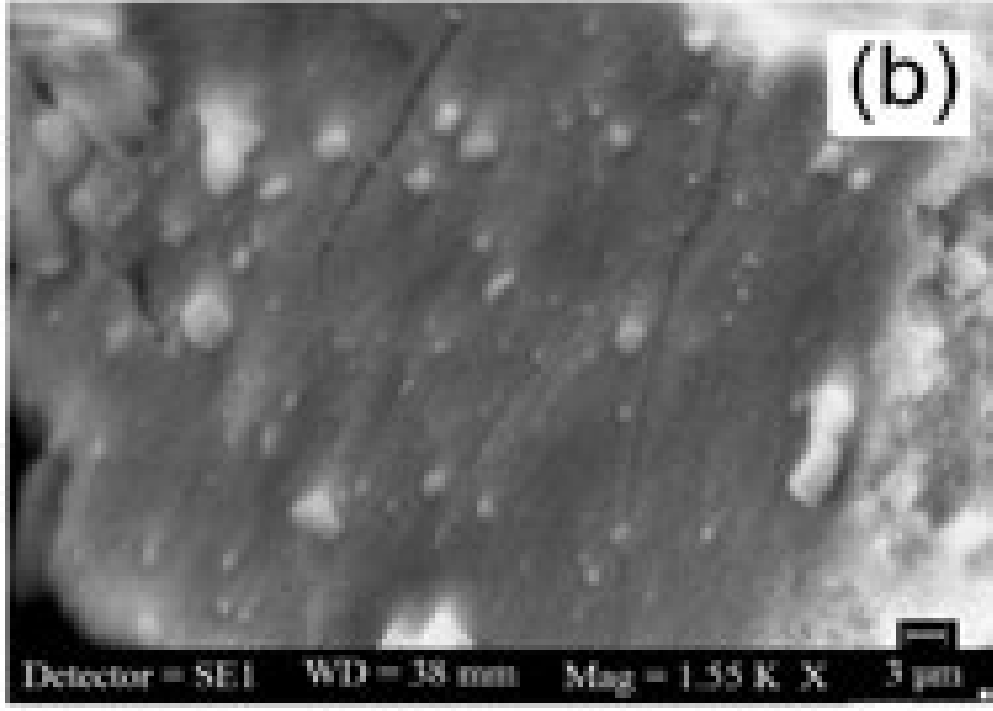

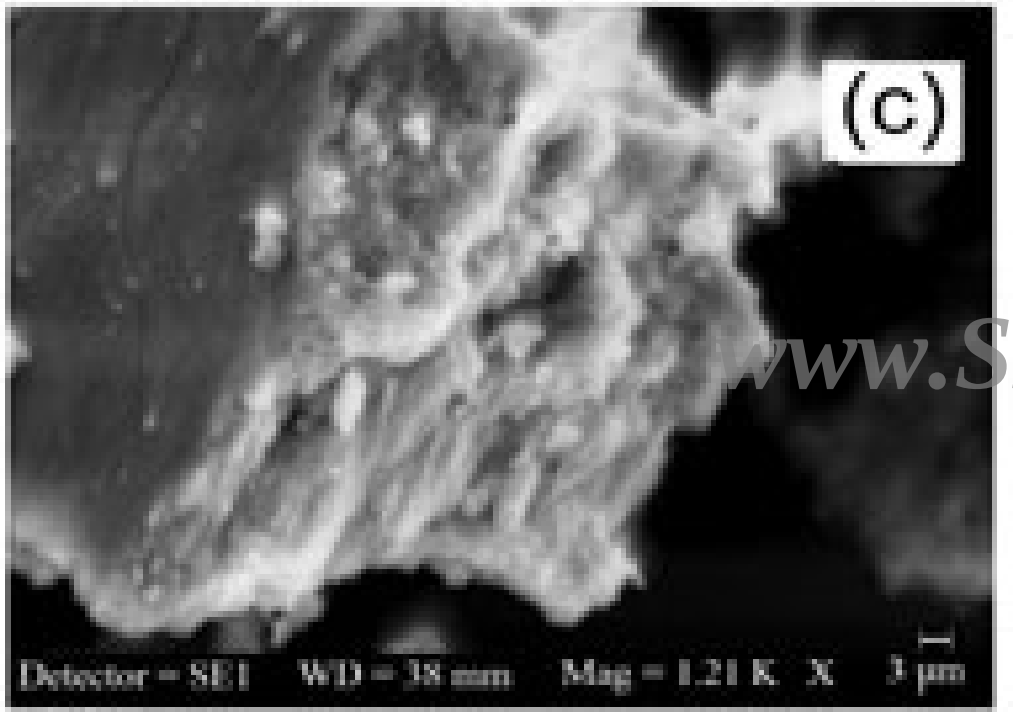

Figure 8

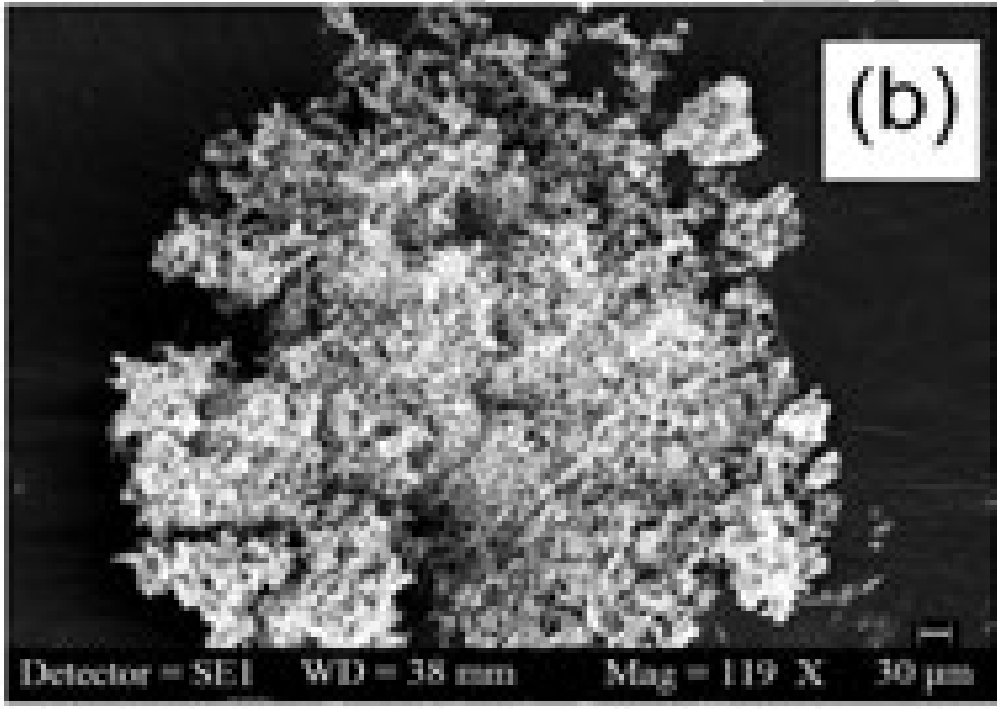

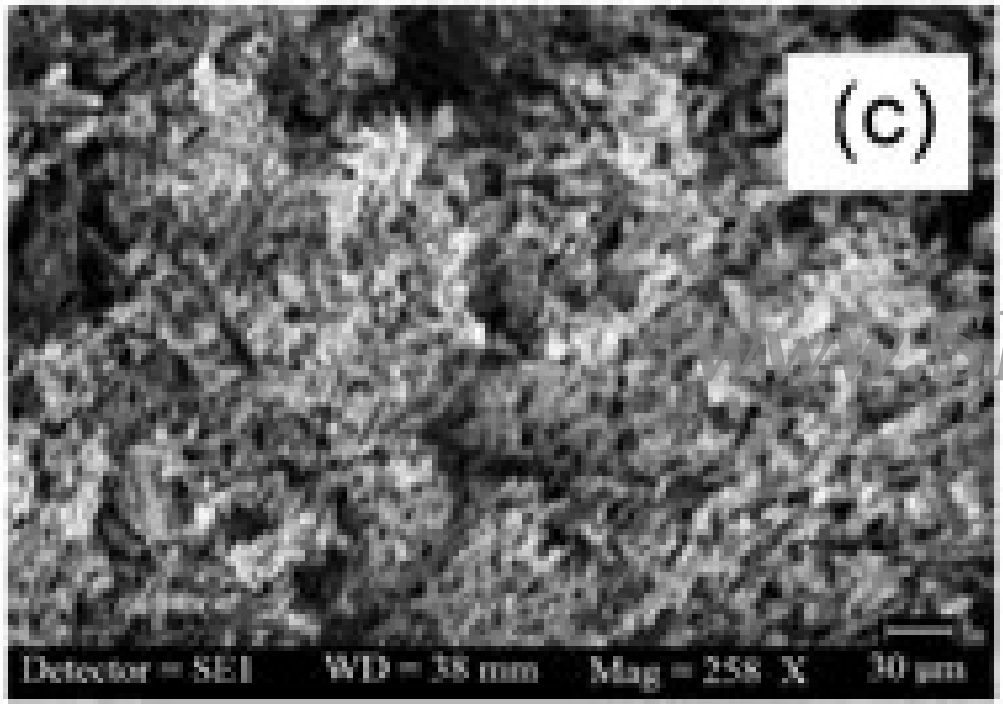

Figure 9

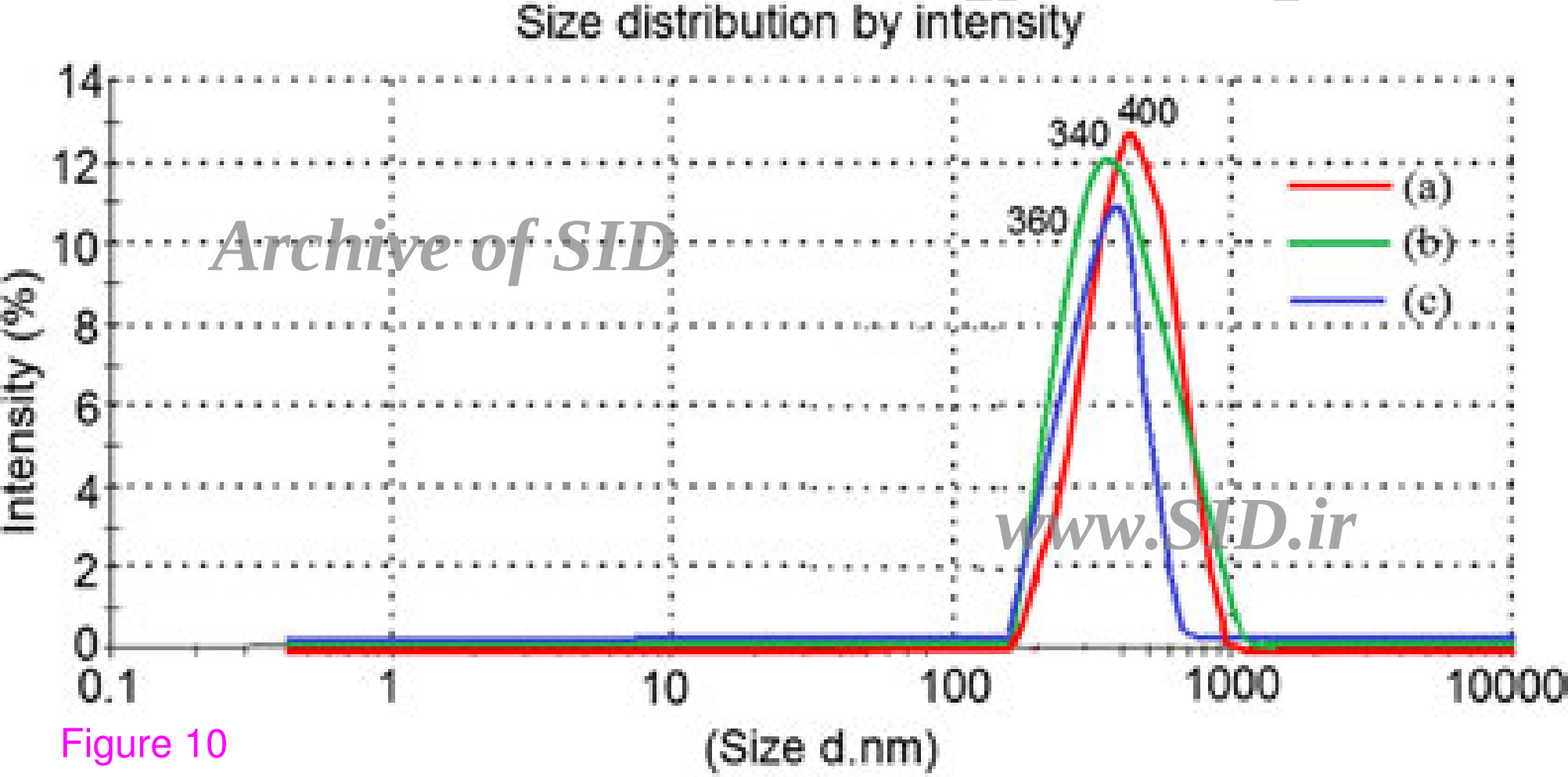
Size distribution by intensity
Intensity (%)
(Size d.nm)
0.1
1
10
100
1000
10000
0
2
4
6
8
10
12
14
340
400
360
(a)
(b)
(c)
Archive of SID
www.SID.ir

Figure 10

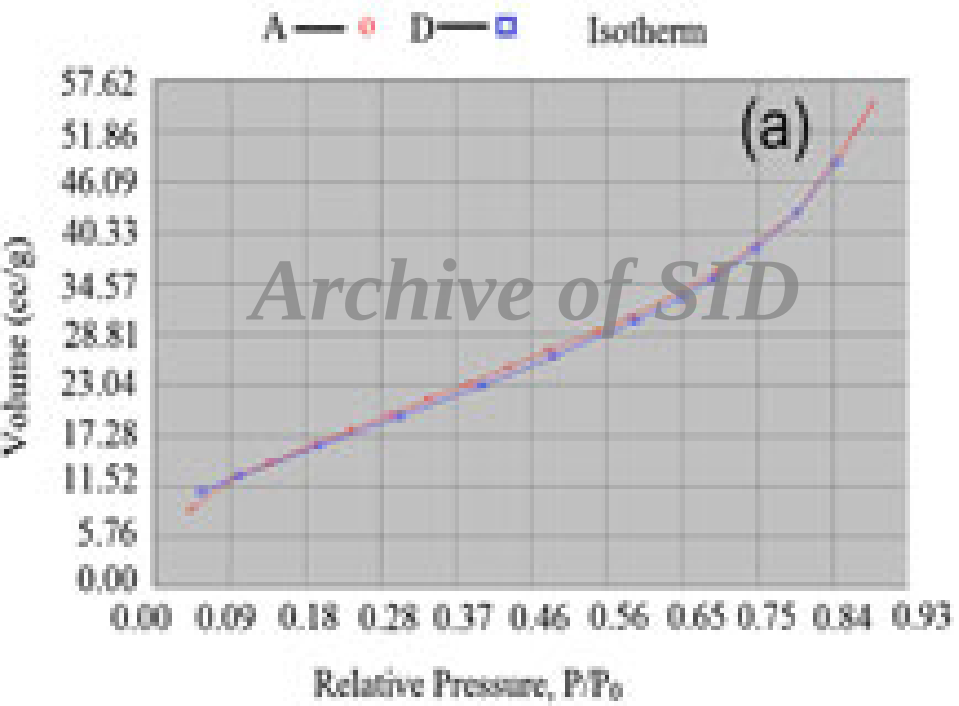

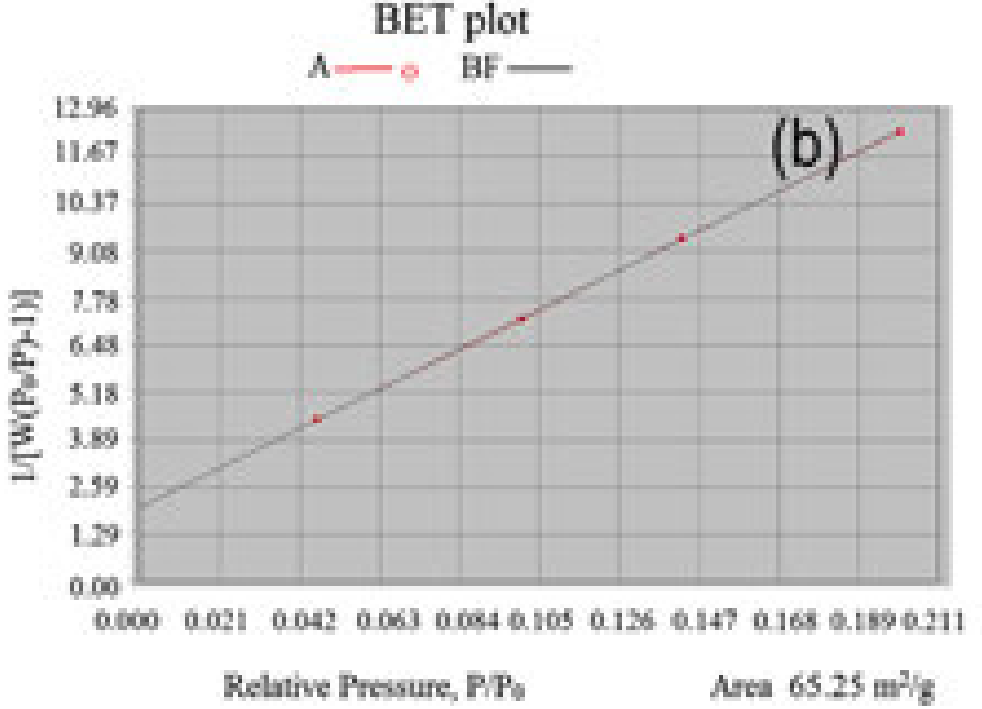

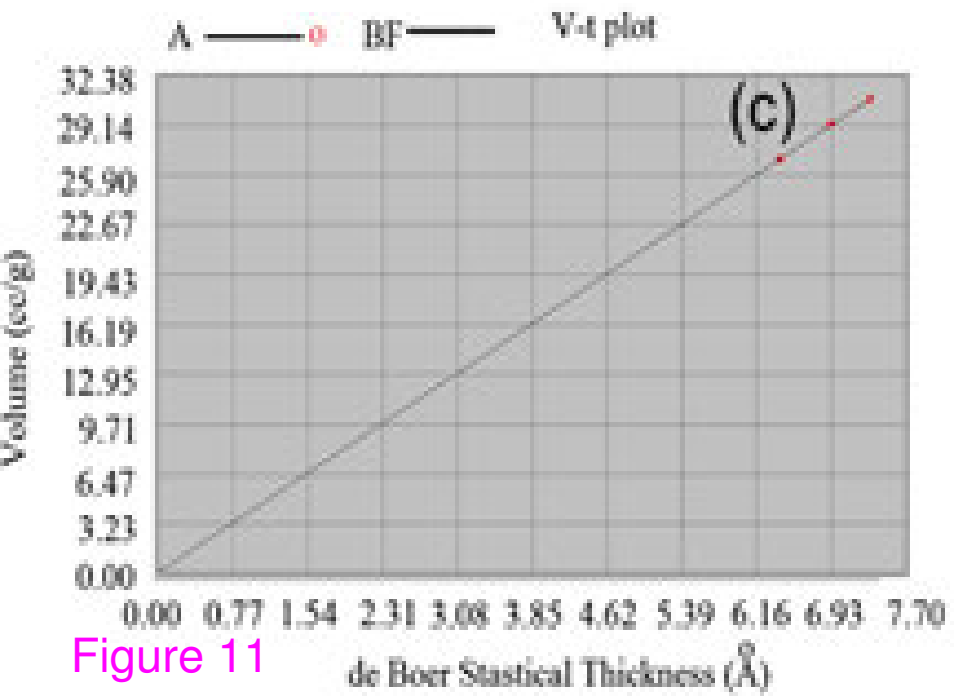

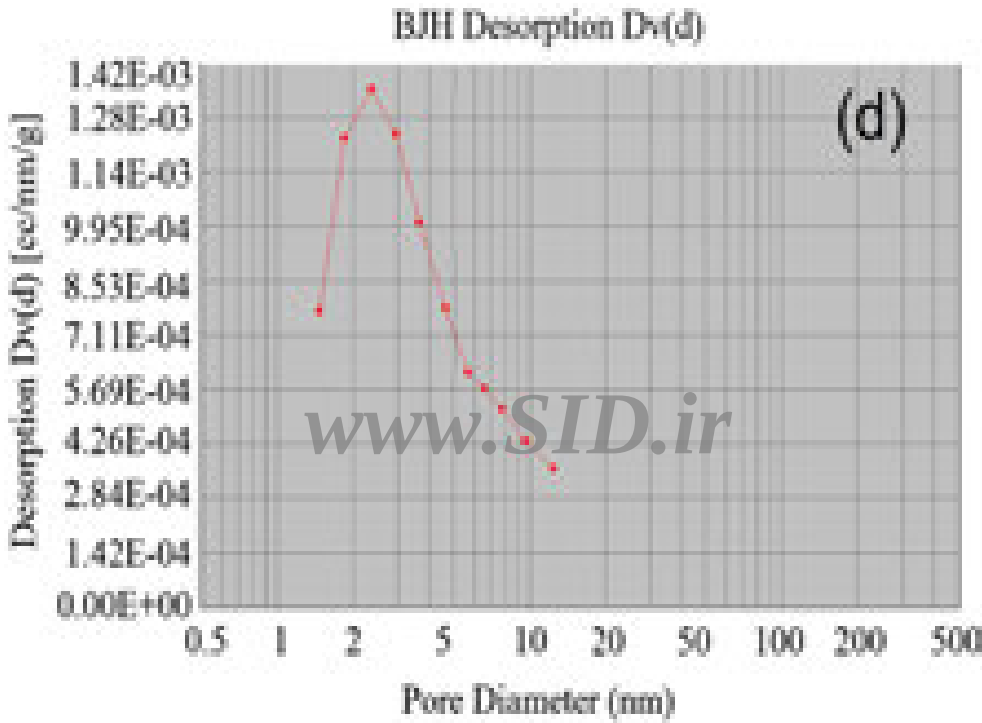

Figure 11